A Journal of the Gesellschaft Deutscher Chemiker

Angewandte International Edition GDCh Chemie

www.angewandte.org

Accepted Article

Title: Photo-thermo catalytic oxidation over TiO2-WO3 supported platinum catalyst

Authors: Leilei Kang, Xiao Yan Liu, Aiqin Wang, Lin Li, Yujing Ren, Xiaoyu Li, Xiaoli Pan, Yuanyuan Li, Xu Zong, Hua Liu, Anatoly I. Frenkel, and Tao Zhang

To be cited as: *Angew. Chem. Int. Ed.* 10.1002/anie.202001701

Link to VoR: https://doi.org/10.1002/anie.202001701

WILEY-VCH

10.1002/anie.202001701

RESEARCH ARTICLE

WILEY-VCH

Photo-thermo catalytic oxidation over TiO_2-WO_3 supported platinum catalyst

Leilei Kang,[a] Xiao Yan Liu,*[a] Aiqin Wang,[a] Lin Li,[a] Yujing Ren,[a],[b] Xiaoyu Li,[a],[b] Xiaoli Pan,[a] Yuanyuan Li,[c] Xu Zong,[d] Hua Liu,[a],[b] Anatoly I. Frenkel,[c],[e] and Tao Zhang*[b],[d]

[a] Dr. L. Kang, Prof. Dr. X. Liu, Prof. Dr. A. Wang, Prof. Dr. L. Li, Dr. Y. Ren, X. Li, X. Pan, H. Liu
CAS Key Laboratory of Science and Technology on Applied Catalysis
Dalian Institute of Chemical Physics, Chinese Academy of Sciences
Dalian 116023, China
E-mail: xyliu2003@dicp.ac.cn

[b] Dr. Y. Ren, X. Li, H. Liu, Prof. Dr. T. Zhang
University of Chinese Academy of Sciences
Beijing 100049, China
E-mail: taozhang@dicp.ac.cn

[c] Dr. Y. Li, Prof. Dr. A. Frenkel
Materials Science and Chemical Engineering Department
Stony Brook University
Stony Brook, New York 11794, United States

[d] Prof. Dr. X. Zong, Prof. Dr. T. Zhang
State Key Laboratory of Catalysis
Dalian Institute of Chemical Physics, Chinese Academy of Sciences
Dalian 116023, China

[e] Prof. Dr. A. Frenkel
Chemistry Division
Brookhaven National Laboratory
Upton, New York 11973 United States

Supporting information for this article is given via a link at the end of the document.

Abstract: Photo-thermo catalysis that integrates photocatalysis on semiconductors with thermocatalysis on supported nonplasmonic metals has emerged as an attractive approach to improve the catalytic performances. However, an understanding of the mechanism from both of the thermo- and photo- catalytic perspectives is missing. Here, the deep insights into the photo-thermo catalysis are achieved *via* the catalytic oxidation of propane (C_3H_8) over the Pt/TiO_2-WO_3 catalyst that severely suffers from the oxygen poisoning at high O_2/C_3H_8 ratios. After introducing ultraviolet-visible light, the reaction temperature for 70% conversion of C_3H_8 is lowered to a record-breaking 90 ^oC from 324 ^oC and the apparent activation energy drops from 130 kJ/mol to 11 kJ/mol. Furthermore, the reaction order of O_2 is -1.4 in dark but reverses to 0.1 under light, which, therefore, suppresses the oxygen poisoning of the Pt catalyst. The underlying mechanism is proposed based on the direct evidences of the *in situ* captured reaction intermediates.

Introduction

Photocatalysis and thermocatalysis have been developed separately with their own principles. While, integrating photo-generated charge carriers with thermocatalysis, namely photo-thermo catalysis, has been developing as a burgeoning field.[1] It is distinguished from the photo-thermal reaction that merely emphasizes the photo-induced heating effect on the reactions.[2] The remarkable advantages that couple the photonic and thermal stimuli over the plasmonic metals (Au, Ag, Cu) have been intensively studied in many typical reactions.[3] By contrast, an in-depth understanding of the photo-thermo catalysis on semiconductor supported nonplasmonic metals (Pt, Pd, Rh, etc.) from both of the thermo- and photo- catalytic point of view is still lacking.

Catalytic oxidation reaction using molecular oxygen as the oxidant is industrially important.[4] Supported platinum is one of the most active catalysts for this kind of reactions. Distinct from the CO poisoning in CO oxidation,[5] the active Pt sites on the surface of the catalysts can be easily poisoned by oxygen in most of the oxidation reactions.[6] For instance, the activity of supported Pt catalysts drops sharply with the augment of O_2/propane (C_3H_8) ratios,[7] which is a pervasive problem in supported platinum group metal (PGM) catalysts for hydrocarbon oxidation.[8]

Herein, the photo-thermo catalysis of semiconductor-supported Pt catalyst (Pt/TiO_2-WO_3) is found to be capable of dramatically enhancing the catalytic oxidation of C_3H_8 at low temperatures and high O_2/C_3H_8 ratio (volume ratio: 20). With the irradiation of ultraviolet-visible light, the reaction temperature for 70 % C_3H_8 conversion (T_{70}) decreases from 324 ^oC to 90 ^oC, correspondingly, the apparent activation energy (E_a) reduces more than ten times. The reaction order (n) of the reactants changes sharply, especially for the O_2 increased from -1.4 to 0.1, thus, the oxygen poisoning of the Pt catalyst can be overcome. The peroxycarbonate (-OCO_3) is found as the intermediate for this reaction for the first time by *in situ* diffuse reflectance infrared Fourier-transform spectroscopy (DRIFTS) and the superoxide anion (O_2^-) is determined as the active oxygen species by *in situ* electron paramagnetic resonance (EPR) under the photo-thermo reaction process. The origin of the synergistic effect between the photo- and thermo- catalysis is proposed. The photo-induced charge carriers promoted by rising temperature are determined as the most important factors that facilitate the activation and desorption of the adsorbed oxygen on the Pt surface.

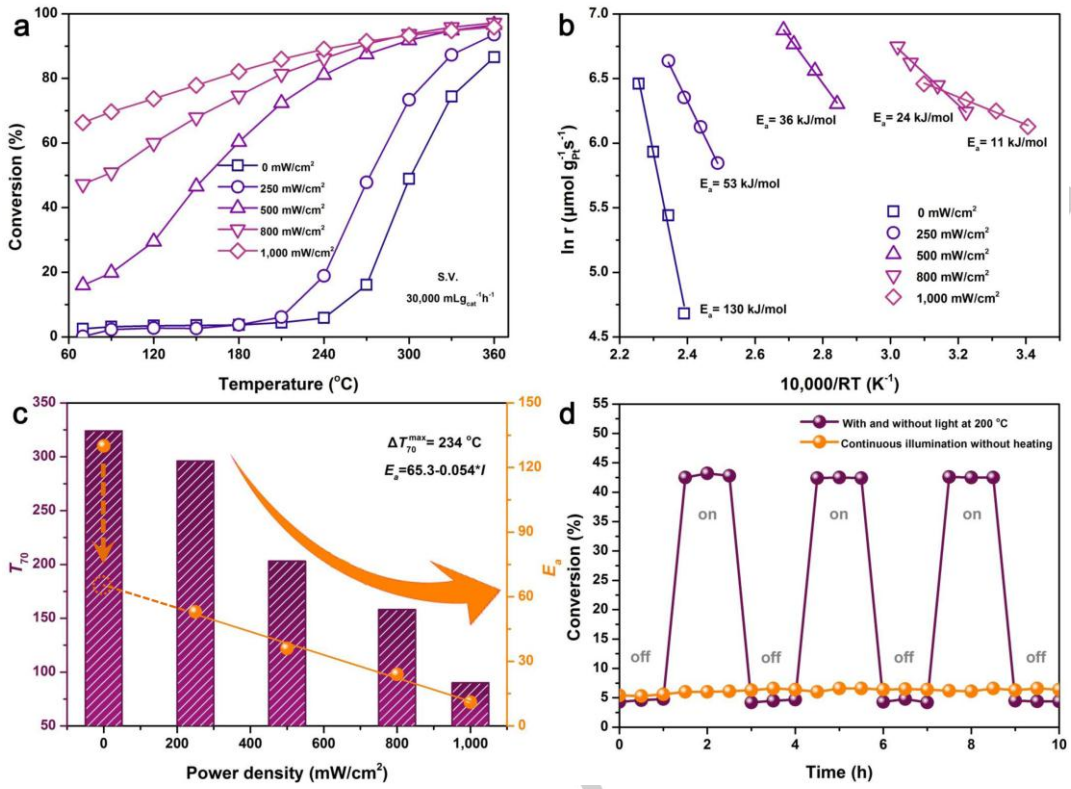

Figure 1. (a) Catalytic activity, (b) Arrhenius plots as well as (c) T_{70} and E_a of the Pt/TiO_2-WO_3 catalyst under light with different power density. (d) C_3H_8 conversion on the Pt/TiO_2-WO_3 catalyst under continuous illumination without heating and at 200 °C with and without light irradiation (power density: 400 mW/cm^2).

Results and Discussion

The Pt/TiO_2-WO_3 catalyst was synthesized by an impregnation method. By balancing both of the light absorption (the results of ultraviolet-visible spectroscopy (UV-vis) in Figure S1) and the specific surface area (the results of N_2 adsorption-desorption isotherms in Figure S2) of the different supports, TiO_2-WO_3 with molar ratio of 1:1 was selected as the support of the catalyst. The loading of Pt in the Pt/TiO_2-WO_3 catalyst was determined to be 0.48% by inductively coupled plasma spectrometer (ICP-AES). Figure S3a shows scanning transmission electron microscopy (STEM) image of the reduced Pt/TiO_2-WO_3 catalyst. The size of Pt clusters dispersed on the TiO_2-WO_3 support is ~0.8 nm. In the energy dispersive spectroscopy (EDS) mappings of Pt, W and Ti elements (Figure S3b), one can see that the distribution of Pt is in accordance with that of W instead of Ti, portending that Pt would preferentially deposit onto the surface of WO_3 because of the relatively better affinity between Pt and WO_3.[9] Moreover, the XRD patterns of the TiO_2-WO_3 support are composed of anatase and rutile TiO_2, and monoclinic WO_3. No obvious diffraction peak of Pt crystal is found, indicating no large Pt nanoparticle in the Pt/TiO_2-WO_3 catalyst (Figure S4).

The catalytic testing was carried out at atmospheric pressure in a self-designed continuous flow fixed-bed quartz reactor, which allows all of the feed gas to go through the catalyst bed. The cross-section of the reactor is profiled in Figure S5. The mass space velocity (S.V.) was 30000 mL g_{cat}^{-1} h^{-1}. The wide passband infrared filter was used in the Xenon lamp to avoid the localized thermal effect of infrared light on the surface of the catalyst. Moreover, the temperature of the catalyst bed was measured by a thermocouple of the furnace so that the light-induced heating can be balanced. Prior to reaction, the catalyst was reduced in flowing hydrogen (10% H_2/He) to improve the activity (Figure S6), since metallic Pt is the most active site for C_3H_8 oxidation.[10] As a contrast, the activity of the TiO_2-WO_3 support is sluggish under the same reaction conditions (Figure S7). Figure 1a shows the light-off curves under light with temperature. It is obvious that the activity of the Pt/TiO_2-WO_3 enhances with the increase of the light intensity. The best performance is achieved when the light intensity is 1000 mW/cm^2. In this case, the reaction temperature for 70% conversion of C_3H_8 (T_{70}) is as low as 90 °C, which is 234 °C lower than that in dark. In addition, no obvious hysteresis can be found in the light-off curves of the fresh and used Pt/TiO_2-WO_3 catalysts, demonstrating the excellent stability (Figure S8).

To get deep insight into the origin of the enhancement, the Arrhenius plot is given in Figure 1b. The E_a of our catalyst is 130 kJ/mol in dark, while it decreases to 11 kJ/mol under strong light. Such a small E_a value is beyond the contribution of thermodynamics. For clarity, these results are summarized in Figure 1c. It is interesting to find that the E_a value is inversely proportional to the power density of the light (I):

$$E_a = 65.3 - 0.054 * I \quad (1)$$

According to this equation, the E_a can be extrapolated to be 65.3 kJ/mol when the light intensity is infinitely close to zero.

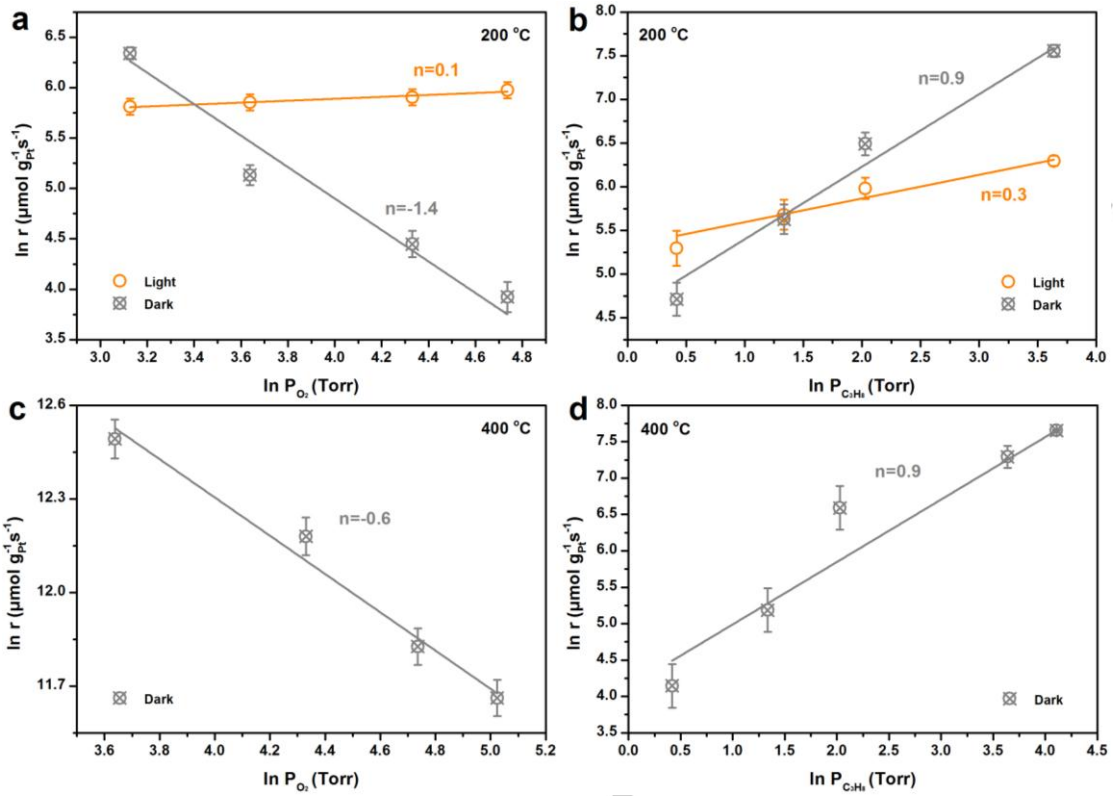

Figure 2. Dependence of reaction rate on partial pressure of (a) O_2 and (b) C_3H_8 at 200 °C with and without light irradiation (power density: 500 mW/cm^2) as well as (c) O_2 and (d) C_3H_8 at 400 °C in dark.

Considering that the E_a is as high as 130 kJ/mol in dark (dashed arrow in Figure 1c), we speculate that the mechanism of the photo-thermo catalysis is different from that of the thermal catalysis. To differentiate the contributions of light and heat, we compared the activities of photocatalysis, thermocatalysis and photo-thermo catalysis, respectively (Figure 1d). Under continuous illumination without heating, the conversion of C_3H_8 merely maintains at ~5%. We further tracked the steady-state reaction at 200 °C with and without light irradiation. The conversion of C_3H_8 under light (on) surges to ~9 times of that in dark (off). Also, the light enhancement process is reproducible. Therefore, the superior activity of the Pt/TiO_2-WO_3 catalyst for catalytic oxidation of C_3H_8 can be attributed to the synergic effect of light and heat. Furthermore, the specific reaction rates based on the Pt content under different conditions are calculated and compared (Table S1). For the Pt/TiO_2-WO_3 catalyst, the specific reaction rate of 457.3 μmol$g_{Pt}^{-1}s^{-1}$ can be achieved at 220 °C in photo-thermo catalysis, which is almost 5 times of the best results reported for supported Pt catalysts (96.44 μmol$g_{Pt}^{-1}s^{-1}$) at the same reaction temperature,[11] even though the light intensity is only 250 mW/cm^2.

To investigate how light and heat influence the reaction, the relationship between the reaction rates and the partial pressure of O_2 and C_3H_8 were measured at 200 °C. It is found that the *n* with respect to O_2 is -1.4 in the absence of light (Figure 2a). The excessive O_2 in the reaction system would speed up the coverage and oxidation of Pt, leading to the degradation of the catalyst. That is, the oxygen can poison the surface of the supported Pt catalyst. However, the *n* changes to 0.1 under light illumination, which means that the reaction rate is almost independent of O_2 concentration under this condition. The *n* of C_3H_8 is 0.9 in dark (Figure 2b), which is consistent with the result of the previous literature.[12] It has been reported that activating C-H bond of hydrocarbon molecule is the kinetically relevant steps (KRS) in catalytic oxidation reaction, which occurs on the metallic Pt surface.[13] This high *n* value mainly originates from the competitive absorption between O_2 and C_3H_8.[14] On the contrary, the *n* of C_3H_8 declines to 0.3 upon light illumination, suggesting that more C_3H_8 molecules can reach the surface of the metallic Pt and be activated.[33] To examine the effect of the possible localized heat on the catalyst surface under light, the dependence of reaction rates on the partial pressure of O_2 and C_3H_8 were further measured at 400 °C in dark. As shown in Figure 2c, the *n* of O_2 is increased to -0.6 in this case, indicating that heating is beneficial for relieving the oxygen poisoning to some extent. Nevertheless, it is still difficult for C_3H_8 molecules to approach to the Pt surface, since the *n* of C_3H_8 still keeps at 0.9 (Figure 2d). The results unambiguously verify that the photo-thermo catalysis is capable of accelerating the KRS of the oxidation reaction by suppressing the poisoning of the supported Pt catalyst by oxygen and improving the accessibility of C_3H_8 molecules.

To monitor the valence state of the Pt in photo-thermo reaction, *in situ* X-ray absorption spectroscopy (XAS) experiment was conducted on the Pt/TiO_2-WO_3 catalyst, in which the content of Pt was increased to 1 wt% and that of W to 4 wt% for better signal noise ratio.[15] As shown in the normalized X-ray absorption near edge structure (XANES) spectra (Figure 3a), the white line intensities of the activated and reacted catalysts are comparable, and slightly higher than that of the Pt foil but lower

than those of the PtO_2 and $Pt(NH_3)_4(NO_3)_2$ and calcined catalyst, suggesting that the Pt was mainly at metallic state during the continuous photo-thermo reaction (Figure S9). The metallic nature of the activated and reacted catalysts can also be verified by the dominant metallic Pt-Pt coordination in the extended X-ray absorption fine structure (EXAFS) spectra (Figure S10) and the corresponding fitting results (Table S2). In comparison with XAS, *in situ* DRIFTS of CO absorption can afford the first hand information on the charges of Pt on the surface of the catalyst.[16] Figure 3b depicts the typical DRIFT spectra of CO chemisorbed on the Pt catalyst with and without light at 20 °C. When the light off, besides the absorption bands of CO gas phase, there is a vibrational stretch at 2083 cm^{-1}, which can be assigned to the oscillation of CO molecules linearly adsorbed on low-coordinated metallic Pt.[17] Upon light illumination, a new band at 2093 cm^{-1} appears accompanied by the decrease of the band at 2083 cm^{-1}, suggesting that the surface of Pt is slightly electron-deficient.[5] The photo-induced thermal effect can be excluded since heating would make the absorption band shift towards low wavenumbers (Figure S11). Therefore, this result demonstrates that the photoexcited electrons can be pumped from the 5d orbital of Pt to the vacant 2π* orbital of CO by the π electron back donation under light, which is responsible for weakening the Pt-CO bond.[18] Besides, the phenomena are reversible with the light on and off, which indicates the photo-induced electron could be produced reversibly. This is in good agreement with the catalytic result in Figure 1d.

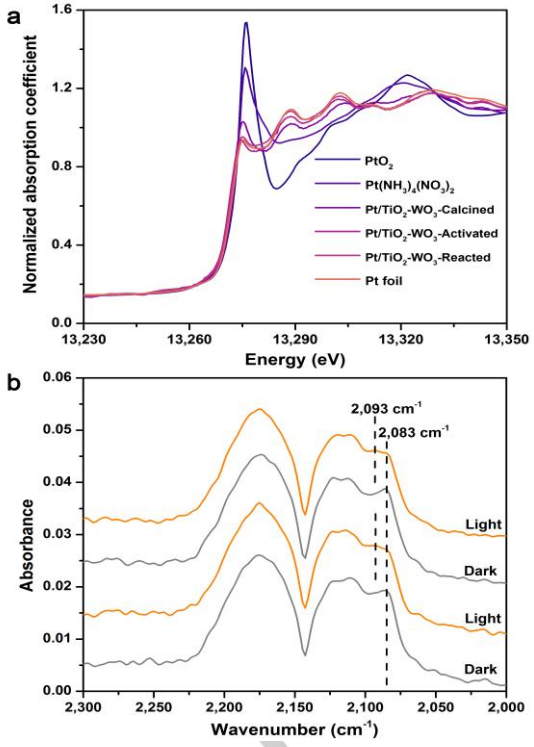

Figure 3. (a) Normalized XANES spectra at the Pt L_{II}-edge of PtO_2, $Pt(NH_3)_4(NO_3)_2$, calcined Pt/TiO_2-WO_3, activated Pt/TiO_2-WO_3, reacted Pt/TiO_2-WO_3 and Pt foil. (b) *In situ* DRIFTS of CO adsorbed on activated Pt/TiO_2-WO_3 at 20 °C with and without light irradiation.

To capture the reaction intermediate, *in situ* DRIFTS of the catalyst in the reaction gas was performed. Figure S12a exhibits the evolution of the DRIFT spectra of the oxygenated carbonaceous species of C_3H_8 oxidation in dark. These bands remain unchanged with time. In contrast, a remarkable new band appears by introducing light illumination, which is highlighted by a red rectangle in Figure S12b. To identify the origin of the band, C_3H_8 and O_2 were successively introduced into the sample cell under light. As shown in Figure 4a, the DRIFT spectrum of the C_3H_8 collected over the catalyst under light is identical to that of the C_3H_8 gas phase.[19] This indicates that the interaction between C_3H_8 and the catalyst is weak, excluding the possibility of the direct activation of C_3H_8 molecules and confirming the participation of O_2 to form the new species. Concurrent with the reduction of IR features of C_3H_8, exhilaratingly, an increasing characteristic band at 1676 cm^{-1} presents in the time-resolved DRIFT spectra in the presence of O_2 (Figure 4b). This newly generated principal band can be ascribed to the stretching vibration of peroxycarbonate in comparison with the $-OCO_3$ band at 1678 cm^{-1} for $(Ph_3P)_2PtOCO_3$.[20] When rising the temperature, the decomposition of the peroxycarbonate can be accelerated, evidenced by the increase of the bands of gaseous CO_2 at 2331 cm^{-1} and 2364 cm^{-1} (Figure 4c). This result definitely confirms that the peroxycarbonate should be the intermediate of the photo-thermo catalytic oxidation of C_3H_8. Serving as the reaction intermediate, peroxycarbonate has been verified by density functional theory (DFT) in CO oxidation on supported Pt cluster.[21]

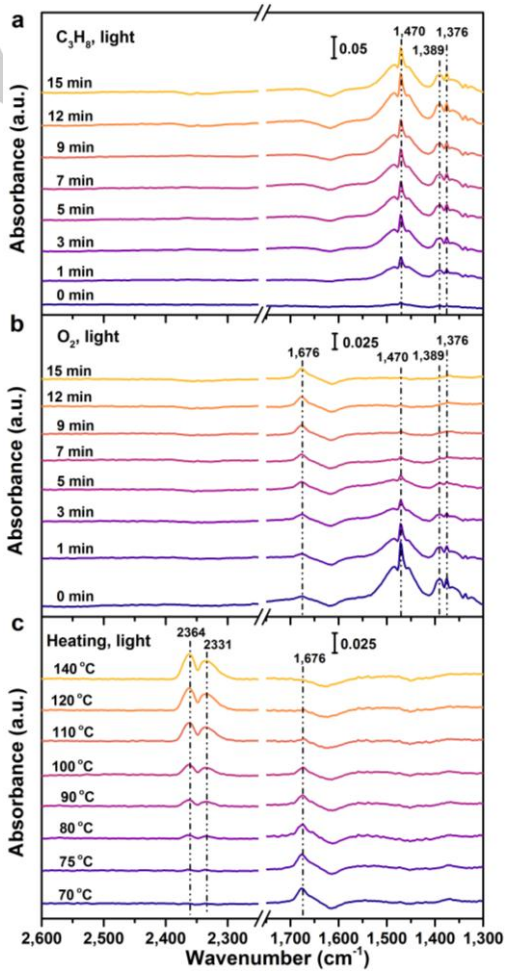

Figure 4. *In situ* DRIFT spectra of the Pt/TiO_2-WO_3 catalyst successively contacted with (a) C_3H_8, (b) O_2 at 70 °C under light illumination and then (c) heated to different temperatures.

The great change of the *n* of O_2 under light suggests that the photo-thermo reaction follows a very distinct pathway, in which light would induce the evolution of oxygen species to drive the reaction. Therefore, identifying active oxygen species is crucial for understanding the underlying mechanism. To this end, EPR was employed, which is a robust technique for detecting unpaired electron.[22] Figure 5a shows the *in situ* EPR spectra obtained at 100 K in air on the reduced Pt/TiO_2-WO_3 with and without light illuminations. In dark, the symmetric signal at g=2.003 is due to unpaired electron trapped at the oxygen vacancies in TiO_2,[23] and the prominent signal at g=1.979 is attributed to Ti^{3+} in the rutile lattice of Degussa P25.[24] Upon continuous illumination for 5 min, a set of paramagnetic superoxide anion O_2^- (g_{xx}=2.002, g_{yy}=2.010, g_{zz}=2.026) signals were observed on the reduced Pt/TiO_2-WO_3 catalyst.[25] Meanwhile, the EPR signals of O_2^- are weakened obviously under light once C_3H_8 is introduced, signifying O_2^- can react with C_3H_8 even at 100 K (Figure 5b). This process is reversible with and without light illumination, further confirming the importance of photo-induced O_2^- in this reaction.

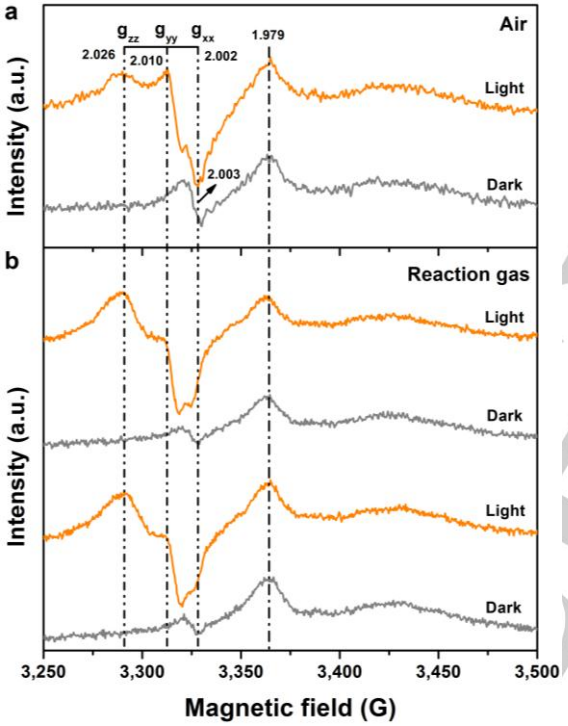

Figure 5. *In situ* EPR spectra of the reduced Pt/TiO_2-WO_3 catalyst in (a) air and (b) reaction gas with and without light irradiation.

The role of WO_3 in our catalyst can also be clarified by EPR measurements. Distinct from the reduced Pt/TiO_2-WO_3, the EPR signals from the reduced Pt/TiO_2 at g=2.026, 2.017 and 2.014 were seen (Figure S13), which can be assigned to O_2^-, O_3^- and O^-, respectively.[26] Compared with the Pt/TiO_2, the exclusive oxygen intermediate (O_2^-) produced on the Pt/TiO_2-WO_3 catalyst should be responsible for its high activity (Figure S14). Besides, a sharp signal at g=1.990 responsible for Ti^{3+} in the anatase lattice appears over the reduced Pt/TiO_2 under light,[55] in parallel with the increase of the signal intensity of Ti^{3+} in the rutile lattice. In this regard, it can be interpreted that the excess photogenerated electrons induce the reduction of Ti^{4+} in Degussa P25 lattice.[26a] The absence of Ti^{3+}, O^- and O_3^- over the Pt/TiO_2-WO_3 should be the evidence of the electron transfer from TiO_2 to WO_3 due to the proper band alignment. To validate this assumption, the photoluminescence (PL) spectra were collected for comparing the ability of charge separation (Figure S15). We can clearly see that the addition of WO_3 can substantially reduce the PL intensity of TiO_2, indicating the suppressed charge recombination. Besides, the participation of WO_3 endows the support with increased utilization of light irradiation (Figure S1).

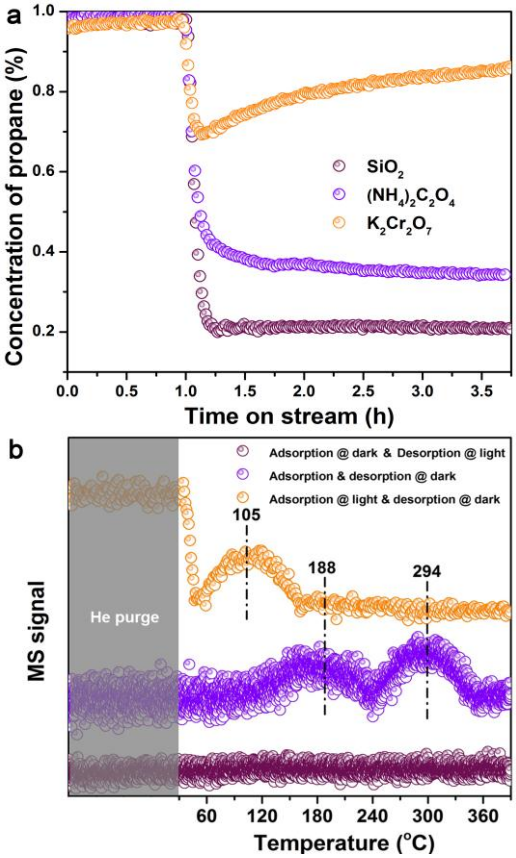

Figure 6. (a) Catalytic activity of the Pt/TiO_2-WO_3 catalyst mixed with SiO_2, $(NH_4)_2C_2O_4$ and $K_2Cr_2O_7$ under light illumination. (b) O_2-TPD profiles of the Pt/TiO_2-WO_3 catalyst under different conditions.

The origination of the photogenerated electrons was studied by comparing the catalytic activities of the Pt/Al_2O_3 with and without light irradiation (Figure S16). Compared with the Pt/TiO_2-WO_3 catalyst (Figure 1a), the catalytic performance of the Pt/Al_2O_3 catalyst under light is slightly better than that in dark, for which the direct photo-excitation of hybridized Pt-O_2 states may be responsible.[27] Besides, the light absorption of the Pt/TiO_2-WO_3 is similar to that of the TiO_2-WO_3 (Figure S17). The above results indicate there is no plasmonic effect over the Pt nanoparticles.[5] Therefore, the electronic effect should be from the TiO_2-WO_3 support. To further verify the contributions of the charge carriers, the potassium dichromate and the ammonium oxalate are used as electron and hole scavengers, respectively.[28] The conversion of C_3H_8 is ~77% when the catalyst was grinded with the inert quartz sand. The trappings of electrons and holes result in the decrease of the equilibrium conversion of C_3H_8 (Figure 6a), respectively. These results

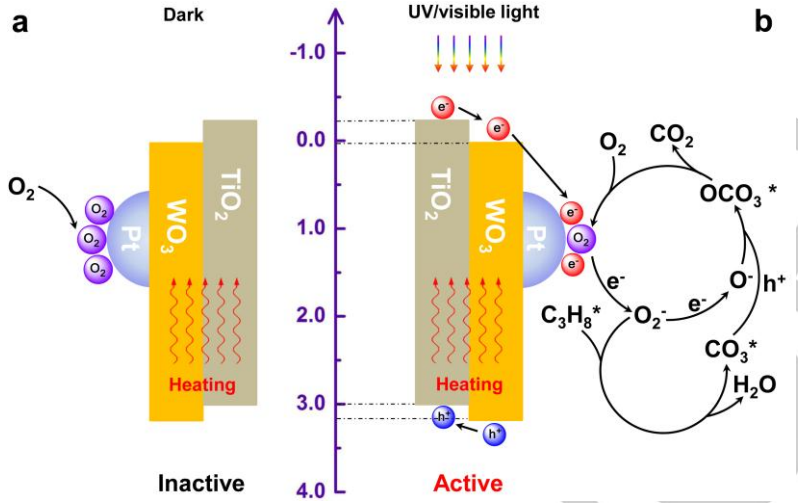

Figure 7. Proposed reaction mechanisms of (a) thermal and (b) photo-thermo oxidation of C_3H_8 over the Pt/TiO_2-WO_3 catalyst at low temperatures.

manifest that the trapping of holes or electrons would inhibit the reaction. In order to understand the activation and desorption of oxygen on the catalyst, the temperature-programmed desorption of O_2 (O_2-TPD) was conducted. As shown in Figure 6b, no O_2 moieties can be detected when the O_2 adsorption process was conducted under light, indicating that light illumination would restrain the O_2 adsorption onto the catalyst. Two prominent peaks appear at around 188 ^oC and 294 ^oC in dark, which correspond to different kinds of the chemically adsorbed O_2* species.[29] In sharp contrast, the O_2* species almost begins to desorb at room temperature and attain the summit at 105 ^oC under light. The baseline drifts downward upon illumination at the beginning, which may stem from the consumption of physically adsorbed O_2. These results clearly suggest that light illumination is helpful for the activation and desorption of oxygen species.

Based on our results, the corresponding mechanisms are proposed. For thermocatalysis, O_2 would preferentially adsorb onto the surface of the active Pt cluster due to the higher affinity, resulting in the oxygen poisoning (Figure 7a). Higher temperature enables the adsorbed oxygen species with high activity, thereby driving the catalytic oxidation reaction. Yet, the excess O_2 would not only suffer competitive adsorption with hydrocarbons but also oxidize the metallic Pt and lead to the low performance of the catalyst.[8a] As illustrated in Figure 7b, photo-thermo catalysis over the Pt/TiO_2-WO_3 catalyst indeed brings about a great change. The O_2 adsorbed onto the Pt surface can be activated to generate anionic superoxide (Pt-O-$O^{\delta-}$) by photogenerated electrons from the semiconductors (*in situ* EPR results in Figure 5a). The active O_2^- species would readily desorb (O_2-TPD results in Figure 6b) and react with the adjacently activated C_3H_8* to produce carbonate (*in situ* EPR results in Figure 5b), followed by the formation of peroxycarbonate with the mediation of holes[30] (*in situ* DRIFT results in Figure 4 a, b). Subsequently, the decomposition of the peroxycarbonate can be accelerated by heating to produce gaseous CO_2 (*in situ* DRIFT results in Figure 4 c) and chemisorbed O_2*. The E_a can be reduced obviously due to the above steps. For improving the reaction rate, suitable heating is of the essence in photo-thermo catalysis. The conductivity of semiconductors increases exponentially with the temperature.[31] We can infer that the elevated temperature may be conductive to transfer more energetic charge carriers to the active sites of the catalyst. From the thermal catalytic point of view, heating would also profit the desorption and/or transform of the intermediates on the catalyst. Thus, the synergy between photocatalysis and thermocatalysis could be reflected.

Conclusion

In summary, photo-thermo catalysis has been demonstrated to be an effective strategy to promote the catalytic oxidation reactivity over the semiconductor supported nonplasmonic metal Pt, especially at low reaction temperatures. The inversely linear dependence of the apparent activation energy on the intensity of light and the great change of the reaction orders unravel the essence of the advantages for the photo-thermo catalytic oxidation reaction, in which overcoming the oxygen poisoning of the supported Pt catalyst is the key factor to accelerate the activation of C-H on Pt surface. The roles of the nonplasmonic metal Pt and the semiconductor support in the catalytic photo-thermal oxidation process are clarified: the decreased electron density of the Pt could enhance the activation of oxygen; while the TiO_2-WO_3 support could not only promote the utilization of the light but could suppress the charge recombination. Combined with the carbonaceous intermediate and active oxygen species detected by the *in situ* characterizations, a new reaction route of the photo-thermo catalysis at low temperatures is proposed, which provides an in-depth insight into the photo-thermo catalysis of the semiconductor supported nonplasmonic metal catalysts.

Acknowledgements

We are grateful for the support from the National Key R&D Program of China (2016YFA0202801), the Strategic Priority Research Program of the Chinese Academy of Sciences (XDB17020400), the National Natural Science Foundation of China (21776271, CSC 201804910082), CAS Interdisciplinary

Innovation Team (BK2018001) and the China Postdoctoral Science Foundation (2017M621171). We also thank the BL 14W beamline at the Shanghai Synchrotron Radiation Facility (SSRF). A. I. F. acknowledges support by the U.S. Department of Energy, Office of Basic Energy Sciences under Grant No. DE-FG02-03ER15476. A. I. F. acknowledges support by the Laboratory Directed Research and Development Program through LDRD 18-047 of Brookhaven National Laboratory under U.S. Department of Energy Contract No. DE-SC0012704 for initiating his research in single atom catalysts.

Keywords: Photo-thermo catalysis • Pt catalyst • semiconductor • oxygen poisoning • reaction order

[1] Z. Wang, H. Song, H. Liu, J. Ye, *Angew. Chem. Int. Edit.* **2019**, 10.1002/anie.201907443.

[2] a) Z. Li, J. Liu, Y. Zhao, G. I. N. Waterhouse, G. Chen, R. Shi, X. Zhang, X. Liu, Y. Wei, X. D. Wen, L. Z. Wu, C. H. Tung, T. Zhang, *Adv. Mater.* **2018**, *30*, 1800527; b) F. Liu, M. Zeng, Y. Li, Y. Yang, M. Mao, X. Zhao, *Adv. Funct. Mater.* **2016**, *26*, 4518-4526; c) X. Meng, T. Wang, L. Liu, S. Ouyang, P. Li, H. Hu, T. Kako, H. Iwai, A. Tanaka, J. Ye, *Angew. Chem. Int. Edit.* **2014**, *53*, 11478-11482; d) W. Gao, R. Gao, Y. Zhao, M. Peng, C. Song, M. Li, S. Li, J. Liu, W. Li, Y. Deng, *Chem* **2018**, *4*, 2917-2928.

[3] a) P. Christopher, H. Xin, A. Marimuthu, S. Linic, *Nat. Mater.* **2012**, *11*, 1044-1050; b) T. H. Tan, J. Scott, Y. H. Ng, R. A. Taylor, K. F. Aguey-Zinsou, R. Amal, *ACS Catal.* **2016**, *6*, 1870-1879; c) C. H. Hao, X. N. Guo, Y. T. Pan, S. Chen, Z. F. Jiao, H. Yang, X. Y. Guo, *J. Am. Chem. Soc.* **2016**, *138*, 9361-9364; d) L. Zhou, D. F. Swearer, C. Zhang, H. Robatjazi, H. Zhao, L. Henderson, L. Dong, P. Christopher, E. A. Carter, P. Nordlander, N. J. Halas, *Science* **2018**, *362*, 69-72; e) X. Guo, C. Hao, G. Jin, H. Zhu, X. Guo, *Angew. Chem. Int. Edit.* **2014**, *53*, 1973-1977.

[4] a) B. Zhao, Y. Jian, Z. Jiang, R. Albilali, C. He, *Chinese J. Catal.* **2019**, *40*, 543-552; b) T. Cai, J. Yuan, L. Zhang, L. Yang, Q. Tong, M. Ge, B. Xiao, X. Zhang, K. Zhao, D. He, *Catal. Sci. Technol.* **2018**, *8*.

[5] Y. Zhou, D. E. Doronkin, Z. Zhao, P. N. Plessow, J. Jelic, B. Detlefs, T. Pruessmann, F. Studt, J. D. Grunwaldt, *ACS Catal.* **2018**, *8*, 11398-11406.

[6] a) B. Y. Xia, H. B. Wu, X. Wang, X. W. Lou, *J. Am. Chem. Soc.* **2012**, *134*, 13934-13937; b) Y. Xu, A. V. Ruban, M. Mavrikakis, *J. Am. Chem. Soc.* **2004**, *126*, 4717-4725.

[7] a) Y. H. Chin, C. Buda, M. Neurock, E. Iglesia, *J. Am. Chem. Soc.* **2011**, *133*, 15958-15978; b) M. Garcia-Dieguez, Y. H. Chin, E. Iglesia, *J. Catal.* **2012**, *285*, 260-272.

[8] a) C. P. O'Brien, G. R. Jenness, H. Dong, D. G. Vlachos, I. C. Lee, *J. Catal.* **2016**, *337*, 122-132; b) W. Tang, W. Xiao, S. Wang, Z. Ren, J. Ding, P. X. Gao, *Appl. Catal. B: Environ.* **2018**, *226*, 585-595.

[9] a) J. G. Santiesteban, D. C. Calabro, W. S. Borghard, C. D. Chang, J. C. Vartuli, Y. P. Tsao, M. A. Natal-Santiago, R. D. Bastian, *J. Catal.* **1999**, *183*, 314-322; b) N. Lei, X. Zhao, B. Hou, M. Yang, M. Zhou, F. Liu, A. Wang, T. Zhang, *ChemCatChem* **2019**, *11*, 3903-3912.

[10] H. Yoshida, Y. Yazawa, T. Hattori, *Catal. Today* **2003**, *87*, 19-28.

[11] a) H. Luo, X.-D. Wu, D. Weng, S. Liu, R. Ran, *Rare Metals* **2017**, *36*, 1-9; b) Y. R. Liu, X. Li, W. M. Liao, A. P. Jia, Y. J. Wang, M. F. Luo, J. Q. Lu, *ACS Catal.* **2019**, *9*, 1472-1481.

[12] T. F. Garetto, E. Rincon, C. R. Apesteguia, *Appl. Catal. B: Environ.* **2004**, *48*, 167-174.

[13] R. Burch, M. J. Hayes, *J. Mol. Catal. A-Chem* **1995**, *100*, 13-33.

[14] Y. Yazawa, H. Yoshida, T. Hattori, *Appl. Catal. A: Gen.* **2002**, *237*, 139-148.

[15] a) X. Liu, M. H. Liu, Y. C. Luo, C. Y. Mou, S. D. Lin, H. Cheng, J. M. Chen, J. F. Lee, T. S. Lin, *J. Am. Chem. Soc.* **2012**, *134*, 10251-10258; b) Y. Tan, X. Y. Liu, L. Zhang, A. Wang, L. Li, X. Pan, S. Miao, M. Haruta, H. Wei, H. Wang, F. Wang, X. Wang, T. Zhang, *Angew. Chem. Int. Edit.* **2017**, *56*, 2709-2713.

[16] B. Qiao, A. Wang, X. Yang, L. F. Allard, Z. Jiang, Y. Cui, J. Liu, J. Li, T. Zhang, *Nat. Chem.* **2011**, *3*, 634-641.

[17] L. DeRita, S. Dai, K. Lopez-Zepeda, N. Pham, G. W. Graham, X. Pan, P. Christopher, *J. Am. Chem. Soc.* **2017**, *139*, 14150-14165.

[18] K. C. Chou, S. Westerberg, Y. R. Shen, P. N. Ross, G. A. Somorjai, *Phys. Rev. B* **2004**, *69*, 153413.

[19] M. A. Hasan, M. I. Zaki, L. Pasupulety, *J. Phys. Chem. B* **2002**, *106*, 12747-12756.

[20] P. Hayward, D. Blake, G. Wilkinson, C. Nyman, *J. Am. Chem. Soc.* **1970**, *92*, 5873-5878.

[21] A. D. Allian, K. Takanabe, K. L. Fujdala, X. Hao, T. J. Truex, J. Cai, C. Buda, M. Neurock, E. Iglesia, *J. Am. Chem. Soc.* **2011**, *133*, 4498-4517.

[22] H. C. Chang, B. Mondal, H. Fang, F. Neese, E. Bill, S. Ye, *J. Am. Chem. Soc.* **2019**, *141*, 2421-2434.

[23] H. Guan, J. Lin, B. Qiao, X. Yang, L. Li, S. Miao, J. Liu, A. Wang, X. Wang, T. Zhang, *Angew. Chem. Int. Edit.* **2016**, *55*, 2820-2824.

[24] N. Siemer, A. Luken, M. Zalibera, J. Frenzel, D. Munoz-Santiburcio, A. Savitsky, W. Lubitz, M. Muhler, D. Marx, J. Strunk, *J. Am. Chem. Soc.* **2018**, *140*, 18082-18092.

[25] H. Sakamoto, T. Ohara, N. Yasumoto, Y. Shiraishi, S. Ichikawa, S. Tanaka, T. Hirai, *J. Am. Chem. Soc.* **2015**, *137*, 9324-9332.

[26] a) N. Siedl, S. O. Baumann, M. J. Elser, O. Diwald, *J. Phys. Chem. C* **2012**, *116*, 22967-22973; b) I. Caretti, M. Keulemans, S. W. Verbruggen, S. Lenaerts, S. Van Doorslaer, *Top. Catal.* **2015**, *58*, 776-782.

[27] M. J. Kale, T. Avanesian, H. Xin, J. Yan, P. Christopher, *Nano Lett.* **2014**, *14*, 5405-5412.

[28] R. Zhang, H. Wang, S. Tang, C. Liu, F. Dong, H. Yue, B. Liang, *ACS Catal.* **2018**, *8*, 9280-9286.

[29] J. J. Li, S. C. Cai, E. Q. Yu, B. Weng, X. Chen, J. Chen, H. P. Jia, Y. J. Xu, *Appl. Catal. B: Environ.* **2018**, *233*, 260-271.

[30] H. Arakawa, K. Sayama, *Catal. Surv. Jpn* **2000**, *4*, 75-80.

[31] W. D. Callister, D. G. Rethwisch, *Materials science and engineering: An introduction*, John Wiley & Sons, New York, **2007**.

10.1002/anie.202001701

Entry for the Table of Contents

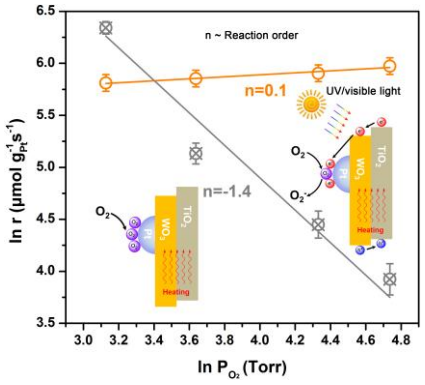

Compared with thermocatalysis, photo-thermo catalytic oxidation of propane (C_3H_8) on Pt/TiO_2-WO_3 catalyst exhibits an excellent activity at high O_2/C_3H_8 ratios and low temperatures. By investigating the apparent activation energy and reaction orders, the enhanced performance can be attributed to breaking through the oxygen poisoning of supported Pt catalyst.